International Journal of Geographical Information Science, 2013
Vol. 27, No. 7, 1453–1468, http://dx.doi.org/10.1080/13658816.2012.705289

Taylor & Francis
Taylor & Francis Group

Measuring the significance of a divide to local drainage patterns

John B. Lindsay[a]* and Jan Seibert[b,c]

[a] *Department of Geography, The University of Guelph, Guelph, Ontario, Canada;* [b] *Department of Geography, University of Zurich, Zurich, Switzerland;* [c] *Department of Physical Geography and Quaternary Geology, Stockholm University, Stockholm, Sweden*

(*Received 24 April 2012; final version received 8 June 2012*)

This article presents a framework for estimating a new topographic attribute derived from digital elevation models (DEMs) called maximum branch length (B_{max}). Branch length is defined as the distance travelled along a flow path initiated at one grid cell to the confluence with the flow path passing through a second cell. B_{max} is the longest branch length measured for a grid cell and its eight neighbours. The index provides a physically meaningful method for assessing the relative significance of drainage divides to the dispersion of materials and energy across a landscape, that is, it is a measure of 'divide size'. B_{max} is particularly useful for studying divide network structure, for mapping drainage divides, and in landform classification applications. Sensitivity analyses were performed to evaluate the robustness of estimates of B_{max} to the algorithm used to estimate flow lengths and the prevalence of edge effects resulting from inadequate DEM extent. The findings suggest that the index is insensitive to the specific flow algorithm used but that edge effects can result in significant underestimation along major divides. Edge contamination can, however, be avoided by using an appropriately extensive DEM.

Keywords: topographic index; ridge; drainage divide; digital elevation models; terrain analysis; fluvial terrain; topography

1. Introduction

Fluvially eroded terrain is characterized by convergent topography, associated with valleys and separated by a series of divergent ridges and drainage divides. Therefore, the basic geomorphic structure of any fluvial landscape can be described by a network of valley bottoms with stream channels and a network of ridges with drainage divides (Mark 1988). These two fundamental networks are interlocking, with the channel network tied to divides at passes and the divide network tied to channel confluences (Werner 1993). Channel and divide networks are both inherently related to the flow of water, sediment, nutrients, contaminants and energy across the terrain (Mark 1988).

Of the two basic landscape networks, channels have received the greatest attention by researchers, in part because of the prominence of drainage network analysis as a tool for examining fluvial processes and basin geomorphic structure (Smart 1978, Wharton 1994, Knighton 1998). Stream ordering is a fundamental concept in network analysis, in which the relative significance of a stream link within the larger river network is determined using

*Corresponding author. Email: jlindsay@uoguelph.ca

a hierarchical system. The most common examples of this type of ordering system are those devised by Horton (1945), later modified by Strahler (1952), and Shreve's (1966) stream magnitude. Stream ordering systems are in common use in hydrological, geomorphological and ecological applications because they provide a simple means of estimating the relative size, with respect to both channel dimensions and discharge, and the relative positioning of individual stream links.

No comparable system for expressing the relative significance or size of drainage divides currently exists or is in widespread use. This is undoubtedly the result of the fact that there is substantial ambiguity in the definition of 'divide size' or 'divide significance'. It is evident that some divides are more significant landscape features than others, for example, a continental divide versus a low ridge that separates flow to adjacent influents on the same headwater stream. It can be difficult, however, to characterize 'divide size' on the basis of morphology. Elevation, for instance, is not a suitable measure, as the divide between major river basins can also include low-lying places or relatively minor divides may be characterized by high local relief. We suggest a measure of divide size that utilizes digital elevation model (DEM)-based flow pathways.

In fluvial landscapes, flow paths that initiate at two nearby locations on a hillslope can be expected to converge after a short distance, except at drainage divides where flow paths initiated on opposite sides of the divide remain separated for comparably long distances. Divides are divergent landscape features, but for minor divides, the divergent flow paths eventually converge at a downstream confluence in the channel or valley bottom network. For larger regional divides, flow paths initiated on either side of the divide may converge at very long distances downstream, and for major divides, the flow paths may never converge, eventually draining to oceans or other major waterbodies via separate river systems. Therefore, the relative significance of a specific location along a divide, or divide size, can be characterized by measuring the distance of separation of flow paths, which we call the *branch length*. The purpose of this article is to describe a new topographic attribute based on the concept of branch length. We propose and evaluate an algorithm for mapping the spatial pattern of *maximum branch length* ($B_{\max}$) based on automated analysis of DEMs.

2. Maximum branch length

Flow paths can be modelled by evaluating the in-flowing and out-flowing connectivity among neighbouring cells within a grid DEM, assuming that the flow paths always follow the surface topography. This topological network of intercell connections forms a group of planar rooted tree graphs known as the local drainage direction network (LDDN) (Burrough and McDonnell 1998). A flow algorithm is a computational procedure that is used to derive the LDDN from an elevation model and to traverse the flow paths contained in the network. LDDNs and flow path tracing are the basis for many topographic attributes and distributed hydrological and geomorphological modelling applications (Moore *et al*. 1991).

Branch length is defined here as the distance along the flow path initiated at a grid cell to the point of intersection (i.e. confluence) with the flow path starting at a second cell. The notation $B_{(k,l)}^{(i,j)}$ is used to represent the branch length measured along the flow path issuing from grid cell (i, j) to its confluence with the flow path issuing from (k, l). This confluence might be a bifurcation in the stream network if the two grid cells are located in different catchments, or a convergent point just a few cells down the flow path, if the two grid cells are part of the same hillslope. Notice that if grid cell (i, j) lies on the downstream flow path of grid cell (k, l), then $B_{(k,l)}^{(i,j)} = 0$. If the two flow paths do not intersect, $B_{(k,l)}^{(i,j)}$ is simply the flow path length from (i, j) to its terminus at the edge of the grid or a cell with undefined flow direction, that is, a pit cell either in a topographic depression or at the edge of a major body of water. This condition occurs along the divide between two basins that drain separately to an ocean, along the divide of an internally drained basin, and where the confluence of interest lies beyond the extent of the DEM and, thus, the LDDN. The last scenario is an edge effect and will be discussed in greater detail later.

Although the definition of $B_{(k,l)}^{(i,j)}$ given above includes any pair of grid cells in a DEM, we will only use the branch length estimated for adjacent cells. In this case, $B_{(k,l)}^{(i,j)}$ can be conceptualized as the downslope distance that a volume of water that is split into two portions by a drainage divide would travel before reuniting. $B_{(k,l)}^{(i,j)}$ can be used as a measure of the significance of the divide between two locations. The value of $B_{(k,l)}^{(i,j)}$ is relatively high where a major regional drainage divide lies somewhere between two test grid cells of the LDDN. It is convenient to assume that the divide between adjacent grid cells in an LDDN is located along the shared edge or corner point between the cells, consistent with a raster representation of a boundary. However, it is important to note that $B_{(k,l)}^{(i,j)}$ is actually assigned to a grid cell and not to the divide inferred to exist between neighbouring cells.

Maximum branch length ($B_{\max}$) is the longest branch length between a grid cell's flow path and the flow paths initiated at each of its neighbours (Figure 1). The pattern of $B_{\max}$ (Figure 2) looks similar to upslope contributing area images. In fact, $B_{\max}$ can be thought of as the complement of contributing area in the same way that the divide network is the complement to the channel network. The contributing area is greatest along valley bottoms and lowest at drainage divides; $B_{\max}$ is greatest at divides and lowest along channels. The presence of a major drainage divide between neighbouring grid cells is apparent in a $B_{\max}$ image as a linear feature of relatively high values (Figure 2).

2.1. Implementation and algorithm description

Although $B_{\max}$ is conceptually simplistic, it is challenging to compute. The calculation of $B_{\max}$ involves the estimation of numerous flow path lengths, which requires an efficient flow algorithm. These algorithms trace flow paths by using the drainage direction data contained in the LDDN to identify the sequence of grid cells that are encountered during a traverse from any interior grid cell to the outlet. A flow path's length can be estimated simply by summing the grid cell flow lengths for each cell in the traverse. It is common to differentiate between the length travelled between cardinal and diagonal neighbours with diagonal flow lengths calculated as $\sqrt{2}$ times the grid resolution.

Our $B_{\max}$ algorithm operates as follows: first, an output grid is created and initialized with zero values. The flow directions in the input LDDN are scanned from the upper left-hand corner to the bottom right-hand corner. For each grid cell (i, j) in the LDDN, branch length is estimated between the cell and four of its neighbours. Specifically, $B_{(i+1,j)}^{(i,j)}$, $B_{(i+1,j-1)}^{(i,j)}$, $B_{(i,j-1)}^{(i,j)}$ and $B_{(i-1,j-1)}^{(i,j)}$ are calculated, that is, the E, SE, S and SW neighbours are considered. The branch lengths between cell (i, j) and the other four neighbouring cells have been calculated during previous scan positions. For each pair of flow paths that must be traversed to estimate the branch lengths, both the length of the (i, j)-flow path to the confluence point and the length of the neighbouring cell flow path to the confluence are measured. If the (i, j)-to-confluence flow path is longer than the current value of cell (i, j) in the output grid, the output grid is updated. The same comparison and update are made for the neighbouring cell.

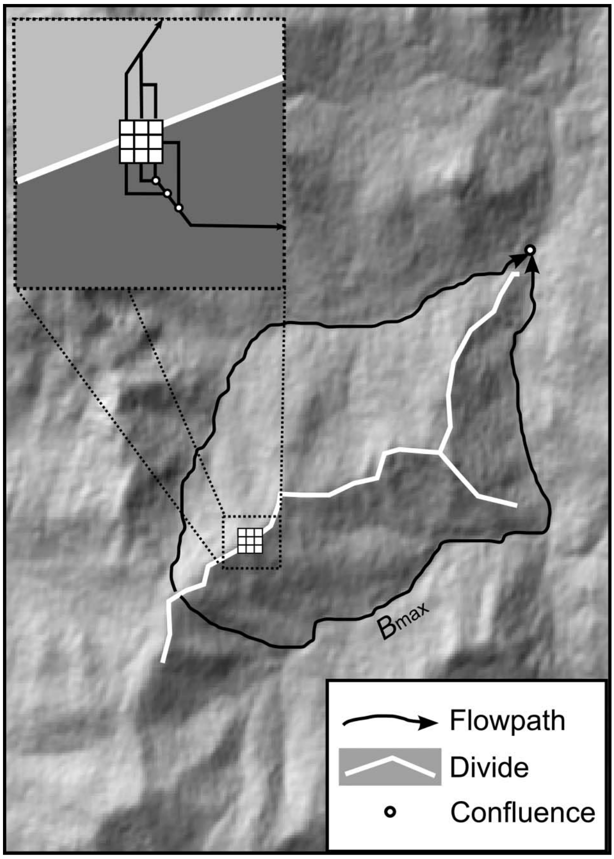

Figure 1. Definition of maximum branch length (B_{max}) for a grid cell located on a drainage divide.

The objective is to identify a downslope confluence point for each pair of neighbouring cells and to measure the length of the two flow paths prior to the confluence. The most straightforward approach to this problem would be to trace one of the flow paths from the starting point all the way to its terminus at the edge of the grid, recording the accumulated flow path length in a temporary grid. The second flow path would then be traced, also measuring flow path length during the traverse, until a non-zero grid cell is encountered in the temporary grid. This approach has the disadvantage that the temporary grid containing the flow paths must be reinitialized with zero values for each branch length measurement. This grid would have to be held in computer memory for efficient calculation, limiting the practical application of this approach to relatively small grids. The second disadvantage of this straightforward approach is that all of the computational effort expended traversing the shared flow path downslope of the confluence is unnecessary. Considering that confluences in the flow paths initiated by most pairs of neighbouring grid cells in an LDDN are likely to occur nearer the start of their flow paths, this simple approach to estimating branch length would be highly inefficient.

To address the first issue, our approach to calculate B_{max} uses two small arrays to store the column and row numbers of each flow path grid cell and the distance along the flow path from the initial grid cell. The length of both arrays is set to twice the diagonal length

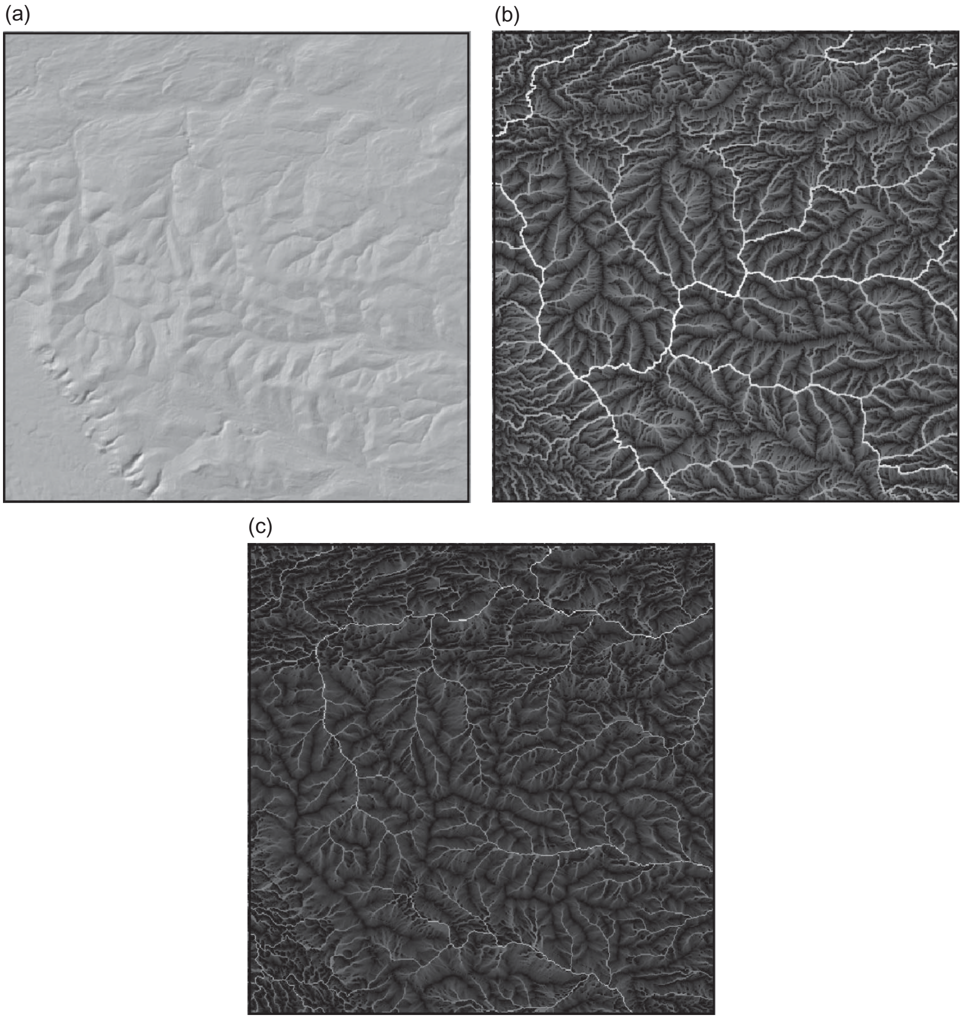

Figure 2. An example DEM (a) and the corresponding patterns of B_{max} (b) and upslope contributing area (c).

of the grid, a value that should be sufficient to accommodate the longest flow path in most LDDNs while having relatively modest computer memory requirements. The second issue is addressed by traversing the two flow paths initiated at neighbouring cells in tandem, with each step searching the flow path arrays for a grid cell in common. This approach does not eliminate unnecessary traverse lengths entirely, unless both flow path branches are an equal number of grid cells long. Scanning flow paths in tandem does, however, significantly reduce the length of redundant traverses and improve algorithm efficiency substantially.

The B_{max} algorithm was implemented using Whitebox Geospatial Analysis Tools (GAT), an open-source geographic information system (GIS). The program, and its source code, can be downloaded from http://www.uoguelph.ca/~hydrogeo/Whitebox/index.html. The algorithm requires an input LDDN that has been derived from a DEM that has had flat areas and topographic depressions removed, a common pre-processing step in flow path-based applications (Burrough and McDonnell 1998).

3. Evaluation of B_{max}

To evaluate B_{max} as a topographic index, we (1) tested its relation to other terrain indices, (2) evaluated the sensitivity to edge effects and (3) investigated the sensitivity to the method used to measure flow lengths.

3.1. Relation to other terrain indices

Numerous terrain indices have been created to describe various characteristics of topography and quantify processes operating in landscapes (Gallant and Wilson 2000). The question is how much new information a novel topographic index can provide. To answer this question, the spatial pattern of B_{max} was compared to several other common terrain indices to evaluate whether B_{max} is redundant or whether it provides additional information about the topographic characteristics of an area. This is particularly relevant given the relation between B_{max} and the pattern of upslope contributing area discussed above.

Statistical analyses were performed to evaluate the associations between B_{max} and various common topographic attributes. Predictors included specific contributing area (SCA), slope gradient (SLOPE), plan curvature (PLANCURV), profile curvature (PROFCURV), tangential curvature (TANCURV) and elevation relative to the nearest channel and drainage divide (RELELEV). A description of each of the indices is given in Table 1 and Gallant and Wilson (2000) give further details on their calculation. These six indices were selected because of their common use in hydro-geomorphic applications. The spatial patterns of B_{max} (Figure 3b) and each of the predictor indices were calculated using a 90-m resolution DEM of the Mad River Basin, Vermont, USA (Figure 3a). The DEM was created from 3-arcsecond Shuttle Radar Topography Mission (SRTM) data. The basin has a relief of nearly 1100 m and is dominated by fluvial processes, which is evident by the well-defined valley network. The statistical distributions of B_{max} and SCA were both found to be highly positively skewed, and therefore, their values were transformed by taking their natural logarithms before the analyses were performed.

A stepwise multiple linear regression analysis was performed to determine whether the variability in B_{max} data could be described using a combination of multiple predictors. For computational reasons, it was not possible to do this analysis on the entire data set, and thus, a randomly drawn sample of 11,531 grid cells (~5% of the number of cells in the image) was used.

Table 1. Descriptions of the topographic indices used in the analyses.

Topographic index	Definition
B_{max}	Maximum length of separation between the flow paths initiated between a grid cell and its neighbours
SCA	Upslope area per unit width of contour
SLOPE	Local steepness
PLANCURV	Rate of change in slope (i.e. curvature) in the contour direction
PROFCURV	Rate of change in slope (i.e. curvature) in the maximum downslope direction
TANCURV	Plan curvature multiplied by slope
RELELEV	Height difference between a location and the first downslope channel grid cell, divided by the height difference between the nearest upslope drainage divide cell and the channel cell, expressed as a percentage

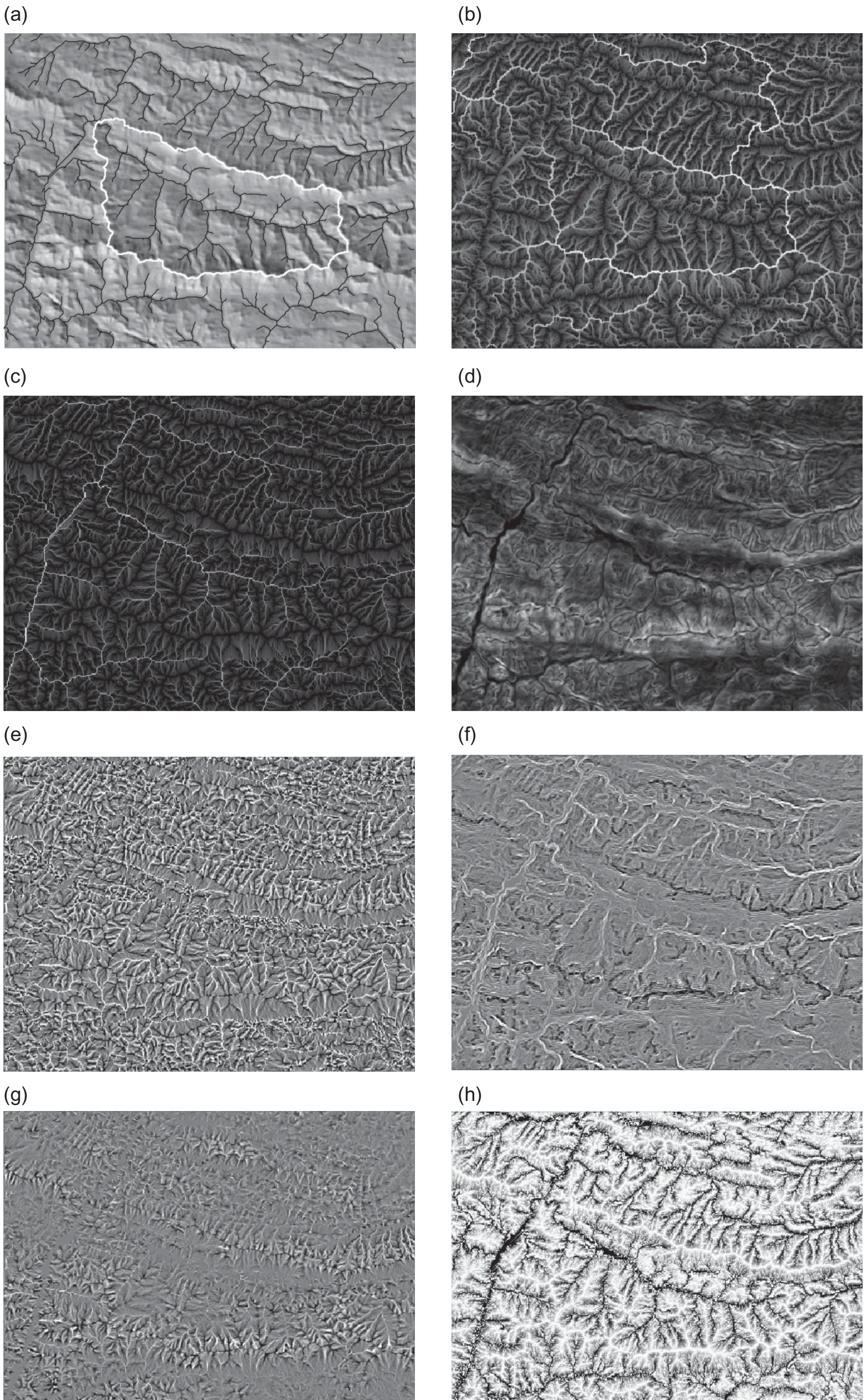

Figure 3. Hillshade image derived from the Mad River Basin 90-m resolution SRTM DEM (a) and derived pattern of $B_{\max}$ (b). Other common DEM-derived topographic attributes including SCA (c), SLOPE (d), PLANCURV (e), PROFCURV (f), TANCURV (g) and RELELEV (h).

3.2. Sensitivity to edge effects

The spatial extent of the DEM, and its derived LDDN, can impact the value of B_{max} that is estimated for a particular grid cell. When neighbouring flow paths are non-convergent (i.e. the flow paths intersect the edge of the LDDN), it is possible that the confluence of their flow paths is located beyond the extent of the LDDN. This scenario is referred to as edge contamination and can potentially influence the estimation of any topographic attribute that is derived using information from an extended neighbourhood around each point in a grid (Gallant and Wilson 2000). Edge contamination usually, but not always, results in an under-estimation of B_{max} values for grid cells that are affected by this phenomenon and affects cells along major drainage divides disproportionately. Not all non-convergent neighbouring flow paths are affected by edge contamination, for example, along divides separating the basins of major rivers that flow to the sea, where non-convergent neighbouring cells are valid.

Edge effects were evaluated using two DEMs of the Mad River Basin DEM. In addition to the 1862-km^2 DEM used in the previous analysis (Figure 3a), a second 15,552-km^2 DEM, possessing the same grid resolution and centred on the same basin, was also used for the analysis. The spatial extent of the second DEM was extended by ~40 km in each direction. Maps of B_{max} were computed for both DEMs and the resulting maps for the overlapping part were compared. Grid cells for which B_{max} was estimated from non-convergent neighbouring flow paths were flagged during the estimation of the topographic attribute as an indicator of the potential extent of this error.

3.3. Sensitivity to the method used to measure flow lengths

There are numerous flow algorithms that can be used to measure flow lengths from grid DEMs (see Gallant and Wilson 2000, Zhou and Liu 2002, Gallant and Hutchinson 2011). These algorithms differ in the way that they construct the LDDN, particularly with respect to the estimation of drainage directions and in the way that they handle dispersion of flow. Although it is computed using a flow algorithm, B_{max} is a topographic attribute based on the determination of the slope lines, or lines of slopes, rather than flow lines (Maxwell 1870, Gallant and Hutchinson 2011). Only one slope line can pass through points of the land surface. Slope lines can be approximated using non-dispersive, or single flow direction, flow algorithms (Wolock and McCabe 1995, Tarboton 1997, Orlandini *et al*. 2003, Orlandini and Moretti 2009).

Since the B_{max} algorithm only requires a non-dispersive LDDN as an input, any non-dispersive flow algorithm can be used to calculate the topographic attribute. However, there are relatively few non-dispersive flow-routing algorithms, which include D8 (O'Callaghan and Mark 1984), Rho8 (Fairfield and Leymarie 1991), Lea's aspect-driven method (Lea 1992) and the D8 modifications described by Orlandini *et al*. (2003, 2009). Of the available algorithms, O'Callaghan and Mark's (1984) D8 method is the simplest and by far the most widely used method. The D8 method assumes that the flow entering a grid cell will be directed to the neighbouring cell with the steepest downward gradient. Since flow directions are based solely on localized 3×3 neighbourhoods and are restricted to multiples of 45°, the D8 method can result in flow path errors, particularly when errors for individual grid cells are accumulated down long flow paths. These errors are often apparent as large areas with parallel drainage directions. This limitation has led to a widespread criticism of the method (Fairfield and Leymarie 1991, Freeman 1991, Tarboton 1997). Nonetheless, D8 is a highly efficient and widely available approach. In fact, very few software packages implement any of the other non-dispersive routing algorithms.

To evaluate the sensitivity of B_{max} to the flow algorithm, the attribute was estimated for the Mad River Basin DEM (Figure 3a) based on LDDNs derived using the D8 and Rho8 algorithms. The Rho8 flow-routing algorithm is a stochastic routing method that attempts to correct for errors caused by D8's preferential assignment of drainage directions (Fairfield and Leymarie 1991). This is accomplished by randomly assigning drainage directions to downslope neighbours, with the probability being proportional to slope. Although individual drainage directions are still restricted to multiples of 45° using the Rho8 method, the accumulated error in drainage directions along a flow path can be substantially reduced, leading to more realistic drainage patterns. The stochastic nature of the Rho8 method, however, results in a different LDDN with each application, which accounts for the relative unpopularity of this algorithm (Burrough and McDonnell 1998). Nonetheless, this routing approach does serve as a useful basis for comparing how sensitive the pattern of B_{max} is to the method used to estimate flow lengths, in recognition that most applications of B_{max} are likely to use the D8 method because of its widespread availability.

4. Results

The algorithm to compute the new topographic index B_{max} was implemented as part of Whitebox GAT. By considering computational efficiency in the implementation, the algorithm was also developed to be capable of processing very large data grids. The authors have used the Whitebox GAT B_{max} algorithm to estimate the index for a 90m resolution data set covering the whole of the US state of Montana, which contained over 60 million grid cells (5954 rows by 10,206 columns). This operation took ~4 hours, using a computer with an Intel Core Duo 2.5 GHz processor and 3.5 GB of memory.

4.1. Relation to other terrain indices

The absolute values of the correlation coefficients for the image correlations between B_{max} and the six other topographic attributes varied between 0.03 and 0.46 (Table 2). All Pearson correlation coefficients in the correlation matrix were found to be statistically significant, which was mainly a result of the large sample size ($N = 230{,}977$). B_{max} was found to be moderately related to TANCURV, RELELEV and PROFCURV, weakly related to SCA and very weakly related to SLOPE and PLANCURV (Table 2). These results suggest that B_{max} provides information that is different from the other tested indices, although several terrain indices are moderately associated with B_{max}.

Table 2. Pearson correlation matrix for seven topographic attributes, including maximum branch length, derived from the Mad River Basin DEM.

Topographic attribute	B_{max}	SCA	SLOPE	PLANCURV	PROFCURV	TANCURV	RELELEV
B_{max}	1.000	−0.376	0.028	−0.027	−0.425	−0.460	0.453
SCA		1.000	−0.174	0.067	0.368	0.518	−0.745
SLOPE			1.000	−0.032	−0.032	−0.082	0.101
PLANCURV				1.000	0.011	0.047	−0.054
PROFCURV					1.000	0.367	−0.524
TANCURV						1.000	−0.452
RELELEV							1.000

The multivariate analysis demonstrated that nearly 34% of the variability in B_{max} ($R = 0.582$, $R^2 = 0.339$, adjusted $R^2 = 0.338$) could be accounted for by a statically significant linear model [$F(4, 11{,}530) = 1181.32$, $P < 0.001$] consisting of five of the predictors, including TANCURV, SCA, RELELEV, PROFCURV and SLOPE. Although the model was found to be significant, most of the variability in B_{max} (66.2%) remained unexplained, thereby supporting the notion that B_{max} provides novel information.

4.2. Sensitivity to edge effects

The patterns of B_{max} derived using the Mad River Basin DEM (Figure 3a) and the more extensive DEM encompassing the same region were in general similar, but B_{max} values were found to be underestimated in the less-extensive grid by several tens of kilometres along the major basin divides (Figure 4a and b). The major basin divides, including part of the Mad River watershed divide, and lesser divides located near the edges of the grid were impacted by edge effects as confluence points were outside the DEM (Figure 4c). This resulted in smaller values for B_{max} in the original DEM compared to the extended DEM (Figure 4a and b). However, none of the features located within the Mad River Basin were affected (Figure 4a and b). This could, of course, be expected as each of the confluences

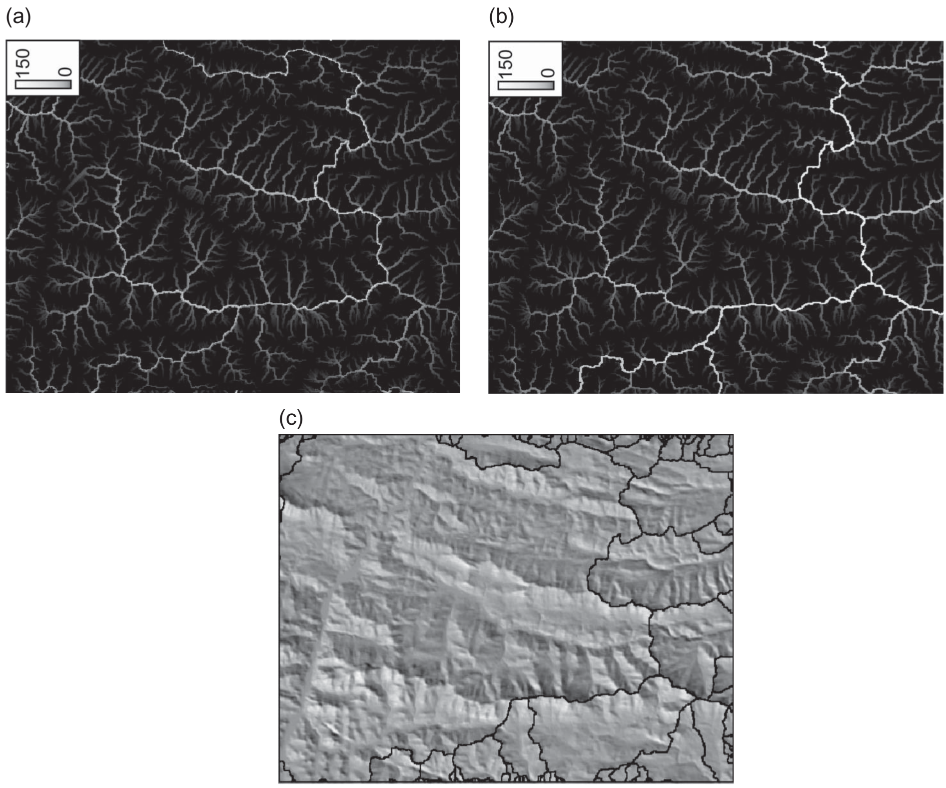

Figure 4. Patterns of B_{max} derived from the original Mad River Basin DEM (a) and a more extensive DEM encompassing the study area (b). Grid cells for which the estimated B_{max} value results from non-convergent neighbouring flow paths overlaid onto a hillshade relief image of the Mad River area (c).

associated with the interior drainage divides was also contained within the basin. It is advisable to use a DEM that extends well beyond the area of interest to estimate B_{max}. The best way to address the edge contamination problem is to use a more extensive DEM, such that all relevant confluence points are included in the analysis.

4.3. Sensitivity to the method used to measure flow lengths

The spatial patterns of B_{max} derived using the D8 (Figure 5a) and Rho8 (Figure 5b) algorithms were found to be nearly identical. Image differencing showed that the differences between the two B_{max} images on a cell-by-cell basis were very small over much of the area (Figure 5c and d). Differences between the images largely occurred due to shifts in individual flow path courses. These positional shifts occurred most frequently along the relatively flat and wide main-stem valley bottom where the random perturbations of drainage directions in the Rho8 method had their greatest effects. These down-valley sites were associated with relatively low B_{max} values (i.e. they were not located along drainage divides). Although positional shifts in flow paths near significant drainage divides were found to occur (e.g. notice the relatively few grid cells in Figure 5c with high values), these shifts were usually never more than one or two grid cells. This explains why the spatial pattern of B_{max} appeared to be largely unaffected by the flow algorithm and is likely to be the case with any flow algorithms. Therefore, B_{max} appears to be relatively insensitive to the method used to estimate flow lengths. This could be confirmed in future work through a comparison of results using the D8-LTD flow algorithm of Orlandini *et al*. (2003). This algorithm eliminates the non-local bias affecting the D8 flow direction method by minimizing the cumulative transverse deviation between steepest slope directions and selected slope directions (Orlandini *et al*. 2003).

5. Discussion

This article describes a novel topographic attribute, B_{max}, which measures the maximum distance travelled along the flow path initiated from a grid cell in an LDDN to the confluence with the flow path initiated at a neighbouring cell. B_{max} can be thought of as the complement of upslope contributing area, a common terrain attribute used in the study of numerous catchment processes and frequently applied to stream and catchment mapping. Although conceptually related to other DEM-derived topographic attributes based on flow-routing techniques, the findings suggest that the spatial pattern of B_{max} is only moderately correlated with other common indices. Moderate-strength correlations are commonly observed among many of the frequently used topographic attributes. It is therefore inferred that B_{max} provides unique and potentially valuable information about landscape structure, particularly related to the organization of drainage divides in regions dissected by river systems.

B_{max} offers a means of quantifying the relative importance of a divide to the pattern of local overland flow paths, that is, the importance of a site with respect to the dispersal of energy and matter across a landscape. Locations on drainage divides that are more distant to their downslope confluence than others are assigned higher B_{max} values. This characteristic of B_{max} provides a convenient basis for assigning a physically meaningful magnitude to divide networks (i.e. a divide's 'size') in much the same way that contributing area and the various stream ordering schemes can be used to assess relative stream size. Focusing study on the organization of drainage divides could lead to insights into landscape structure that are complementary to previous work in the field of drainage network analysis

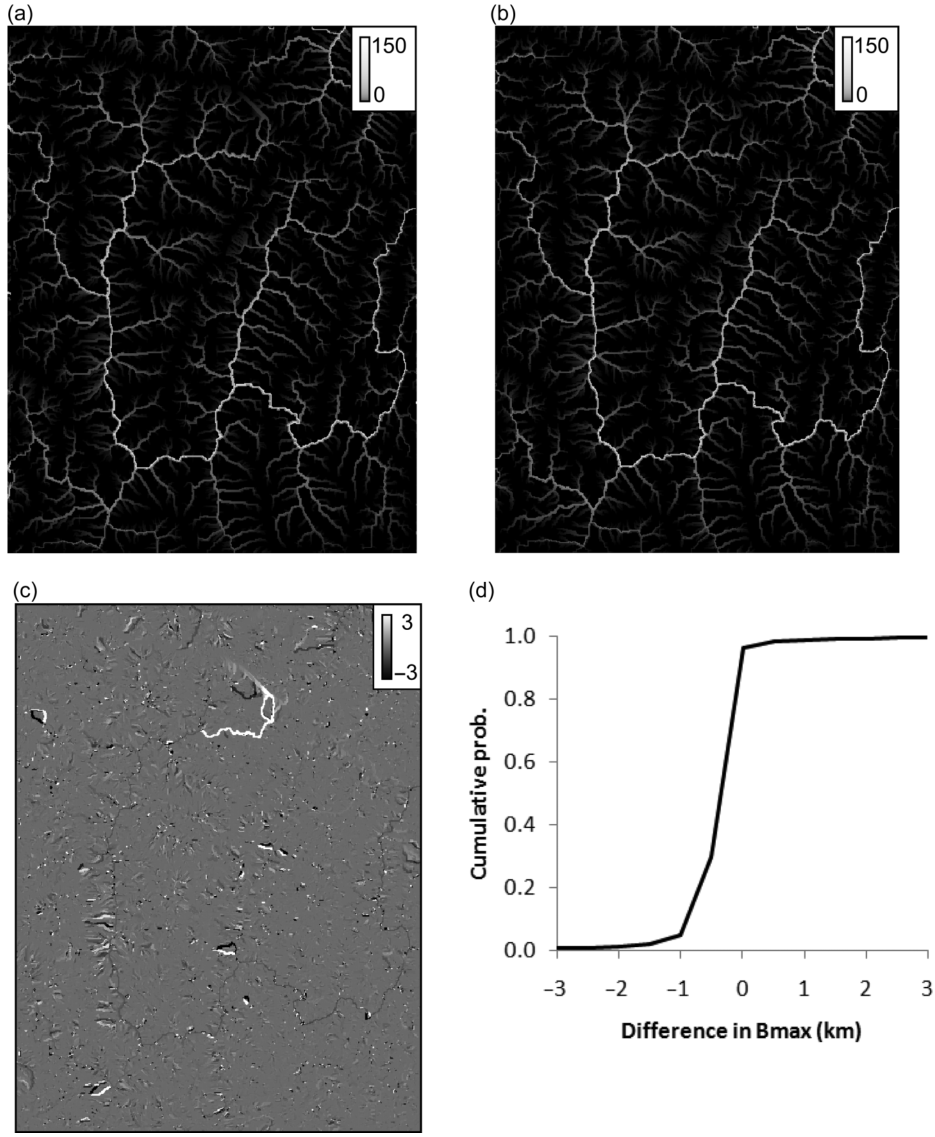

Figure 5. Patterns of $B_{\max}$ derived using the D8 (a) and Rho8 (b) flow-routing methods. The spatial pattern resulting from differencing the two $B_{\max}$ images (c) and the cumulative probability distributions of differenced values (d).

(Wharton 1994). Although there has been some previous research in this area, notably with the work of Cayley (1859), Werner (1972a, 1972b, 1982, 1988, 1991, 1993), Mark (1979, 1982, 1988) and more recently Rana (2006), relatively little attention has been paid to divides in the literature. This may in part reflect the greater topological complexity of divide networks compared to their channel counterparts, as well as the lack of a consistent means of quantifying divide size as a basis for assigning hierarchical structure.

There is an inherent asymmetry in estimating divide size because the distance to a downslope confluence is usually unequal on either side of the divide. That is, the importance of a divide to local drainage patterns depends on which side of the divide you consider. $B_{\max}$ exhibits this asymmetry on either side of a drainage divide because $B_{(k,l)}^{(i,j)} \neq B_{(i,j)}^{(k,l)}$. For many applications, this property of the topographic attribute is likely to be useful and is physically realistic. However, if the information about the asymmetrical characteristic of divide magnitude is deemed not to be desirable in a study (e.g. if the interest in the index is solely for the purpose of mapping divide features), a symmetrical definition of $B_{\max}$ can be applied such that the index reflects the sum of both cells' branch lengths, that is, $B_{(k,l)}^{(i,j)} + B_{(i,j)}^{(k,l)}$. For convenience, both the asymmetrical and symmetrical definitions of the index can be specified in the Whitebox GAT software.

The spatial distribution of $B_{\max}$ does not vary systematically upslope or downslope, unlike the pattern of contributing area, which increases monotonically downstream by a step function. The point along a sub-basin's divide that coincides with the longest flow path will be associated with a local maximum in the $B_{\max}$ distribution. Multiple local maxima are, however, possible along a single sub-basin's divide. Local minima in the index tend to be associated with passes. Although $B_{\max}$ does not vary systematically along divides, the value at any location does tend to be similar to nearby locations except at junctions in the divide network. These sites often coincide with stepped increases in $B_{\max}$ in the same way that confluences in the stream network result in large increases in contributing area. This characteristic is in fact one of the reasons that the spatial patterns of the two terrain attributes look similar.

The value of $B_{\max}$ is often several orders of magnitude lower along hillslopes and channels than it is at ridges. Thus, ridges can be effectively mapped from $B_{\max}$ images using a threshold just as channels are often mapped using contributing area images and a threshold value (Figure 6). This approach can provide more suitable ridge network maps than those that are produced by other common methods that have been proposed including the identification of grid cells with very small contributing areas (Skidmore 1990, Burrough and McDonnell 1998), the identification of cells with high contributing area values derived from an inverted DEM (MacMillan *et al*. 2000) and various morphologically based approaches that apply spatial filters (e.g. Peucker and Douglas 1975, Skidmore 1990, Rana 2006). Ridge networks that are extracted from $B_{\max}$ images are continuous, with the exceptions of a few breaks that occur near the furthest downslope portions of the ridge networks. Most other methods require substantial post-processing to yield unbroken divide networks.

Although $B_{\max}$ is clearly most relevant for sites located along drainage divides, it is estimated for every grid cell in a DEM. For non-divide cells, $B_{\max}$ is essentially a measure of the degree of dispersion in the downstream flow paths passing through an area. This characteristic may be useful for certain applications, for example, landform classification. A related topographic attribute, total branch length (B_{total}), defined here as the sum total of the eight branch lengths for a grid cell and its eight neighbouring cells, may be more suitable when an index of downstream flow dispersion is needed. The branch length tool implemented in the Whitebox GAT software can also measure B_{total}.

Like other DEM-derived topographic indices, $B_{\max}$ is a general property of topographic surfaces. As such, several different approaches and topographic data structures could be used to estimate the attribute. In fact, although the definition in this article assumes that the surface data used to estimate $B_{\max}$ is in a raster grid format, the topographic attribute could be calculated using other data structures such as triangular irregular networks, contour-based DEMs or hexagonally gridded DEMs.

We suggest that branch length, as a measure of divide size, has the potential to be used in several ways. $B_{\max}$ can be used to rank the importance of divides, where a correct determination of divides is most important. It may also be used to map ridges

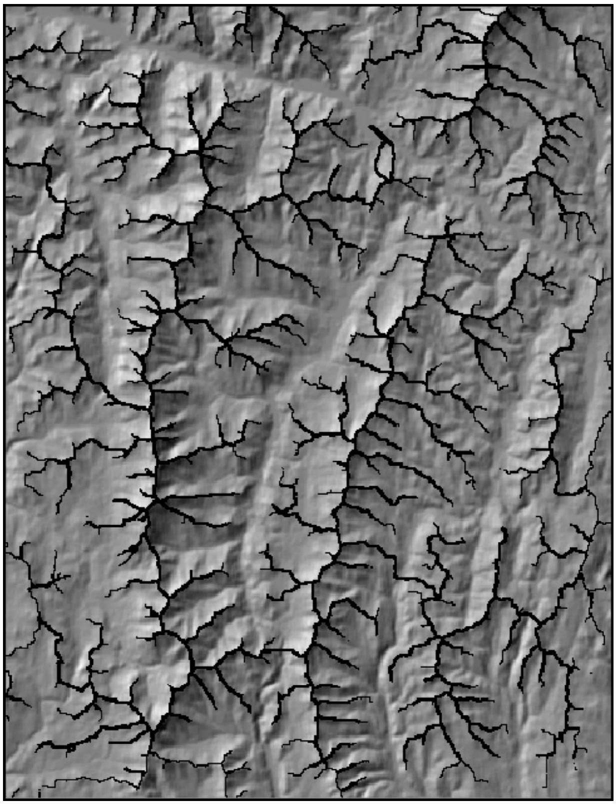

Figure 6. Drainage divide network derived by identifying all grid cells with B_{max} values >3 km.

within fluvial dissected landscapes. In addition, B_{max} provides a measure of dispersion that considers not only the neighbouring cells but also downslope conditions in a similar way to the downslope index (Hjerdt *et al*. 2004). As a dispersion measure, B_{max} might be used in studies related to the transport of contaminants, especially when the contaminant is applied to larger areas such as in the case of airborne pollutants. As a measure of divide size, B_{max} might be useful when fields of climatic variables such as precipitation are generated for hydrological modelling. With increasing divide size, it becomes more important that the corresponding gradients in the climatic fields are estimated correctly. Similarly, with increasing divide size, differences between watershed divides and political boundaries become more important.

6. Conclusions

The following general conclusions can be drawn from this work:

(1) B_{max} provides a potentially useful means for studying the structure of fluvial landscapes with emphasis on the organization of drainage divide in a region. The terrain attribute may be useful in landform classification and ridge mapping applications.
(2) A general framework for computing B_{max} and other related indices based on the notion of branch length has been provided along with an example implementation

in an open-source GIS software package. Particular consideration has been given to improve algorithm performance, given the computationally intensive characteristic of any B_{max} implementation and the need to process massive topographic data sets.

(3) The pattern of B_{max} was found to be relatively insensitive to the flow-routing algorithm used to measure flow lengths, although it is necessary to use a non-dispersive algorithm. The topographic attribute was, however, found to be sensitive to DEM spatial extent. The problem of edge contamination can be lessened, or avoided altogether, by estimating B_{max} using a DEM that is extensive enough to encompass all of the downstream confluences of the divide features in the area of interest. As such, any B_{max} algorithm must be implemented in a way that it is capable of handling very large data sets.

Acknowledgements

The authors acknowledge financial support provided by the Natural Sciences and Engineering Research Council of Canada and the lidar data sets provided by the Ontario Ministry of Agriculture, Food and Rural Affairs. The authors are also thankful for the insightful comments of Stefano Orlandini and the anonymous reviewers, which have served to greatly strengthen this article.

References

Burrough, P.A. and McDonnell, R.A., 1998. *Principles of geographical information systems*. New York: Oxford University Press, 352pp.

Cayley, A., 1859. On contour lines and slope lines. *Philosophical Magazine*, 18, 264–268.

Fairfield, J. and Leymarie, P., 1991. Drainage networks from grid digital elevation models. *Water Resources Research*, 27 (5), 709–717.

Freeman, T.G., 1991. Calculating catchment area with divergent flow based on a regular grid. *Computers and Geoscience*, 17 (3), 413–422.

Gallant, J.C. and Hutchinson, M.F., 2011. A differential equation for specific catchment area. *Water Resources Research*, 47 (5), W05535. doi:10.1029/2009WR008540.

Gallant, J.C. and Wilson, J.P., 2000. Primary topographic attributes. *In*: J.P. Wilson and J.C. Gallant, eds. *Terrain analysis, principles and applications*. New York: John Wiley & Sons, 51–85.

Hjerdt, K.N., *et al*., 2004. A new topographic index to quantify downslope controls on local drainage. *Water Resources Research*, 40 (5), W05602. doi:10.1029/2004WR003130.

Horton, R.E., 1945. Erosional development of streams and their drainage basins: hydrophysical approach to quantitative morphology. *Geological Society of America Bulletin*, 56, 275–370.

Knighton, D., 1998. *Fluvial forms and processes: a new perspective*. London: Arnold Publishing, 383pp.

Lea, N.J., 1992. An aspect-driven kinematic routing algorithm. *In*: A.J. Parsons and A.D. Abrahams, eds. *Overland flow: hydraulics and erosion mechanics*. London: UCL Press, 393–407.

MacMillan, R.A., *et al*., 2000. A generic procedure for automatically segmenting landforms into landform elements using DEMs, heuristic rules and fuzzy logic. *Fuzzy Sets and Systems*, 113, 81–109.

Mark, D.M., 1979. Topology of ridge patterns: randomness and constraints. *Geological Society of America Bulletin Part 1*, 90, 164–172.

Mark, D.M., 1982. Topology of ridge patterns: possible physical interpretations of the "minimum spanning tree" postulate. *Geology*, 9, 370–372.

Mark, D.M., 1988. Network models in geomorphology. *In*: M.G. Anderson, ed. *Modeling geomorphological systems*. New York: John Wiley & Sons, 73–96.

Maxwell, J.C., 1870. On hills and dales. *Philosophical Magazine*, Series 4, **40** (269), 421–425.

Moore, I.D., Grayson, R.B., and Ladson, A.R., 1991. Digital terrain modelling: a review of hydrological, geomorphological, and ecological applications. *Hydrological Processes*, 5, 3–30.

O'Callaghan, J.F. and Mark, D.M., 1984. The extraction of drainage networks from digital elevation data. *Computer Vision, Graphics, and Image Processing*, 28 (3), 323–344.

Orlandini, S. and Moretti, G., 2009. Determination of surface flow paths from gridded elevation data. *Water Resources Research*, 45 (3), W03417. doi:10.1029/2008WR007099.

Orlandini, S., *et al*., 2003. Path-based methods for the determination of nondispersive drainage directions in grid-based digital elevation models. *Water Resources Research*, 39 (6), 1144. doi:10.1029/2002WR001639.

Peucker, T.K. and Douglas, D.H., 1975. Detection of surface specific points by local parallel processing of discrete terrain elevation data. *Computer Graphics and Image Processing*, 4, 375–387.

Rana, S., 2006. Use of plan curvature variations for the identification of ridges and channels on DEM. *In*: A. Riedl, W. Kainz, and G.A. Elmes, eds. *Progress in spatial data handling*. New York: Springer, 789–804.

Shreve, R.L., 1966. Statistical law of stream numbers. *Journal of Geology*, 75, 178–186.

Skidmore, A.K., 1990. Terrain position as mapped from a gridded digital elevation model. *International Journal of Geographical Information Systems*, 4 (1), 33–49.

Smart, J.S., 1978. The analysis of drainage network composition. *Earth Surface Processes and Landforms*, 3, 129–170.

Strahler, A.N., 1952. Hypsometric (area-altitude) analysis of erosional topography. *Geological Society of America Bulletin*, 63, 1117–1142.

Tarboton, D.G., 1997. A new method for the determination of flow directions and upslope areas in grid digital elevation models. *Water Resources Research*, 33, 309–319.

Werner, C., 1972a. Graph-theoretical analysis of ridge patterns. *In*: W.P. Adams and F.M. Helleiner, eds. *International geography*. Montreal: University of Toronto Press, 943–945.

Werner, C., 1972b. Channel and ridge networks in drainage basins. *Proceedings of the Association of American Geographers*, 4, 109–114.

Werner, C., 1982. Analysis of length distribution of drainage basin perimeter. *Water Resources Research*, 18, 997–1005.

Werner, C., 1988. Formal analysis of ridge and channel patterns in maturely eroded terrain. *Annals of the Association of American Geographers*, 78 (2), 253–270.

Werner, C., 1991. Several duality theorems for interlocking ridge and channel network. *Water Resources Research*, 27, 3237–3247.

Werner, C., 1993. Ridge/channel path interdependence in drainage basins. *Geografiska Annaler Series A, Physical Geography*, 75 (3), 73–81.

Wharton, G., 1994. Progress in the use of drainage network indices for rainfall-runoff modelling and runoff prediction. *Progress in Physical Geography*, 18 (4), 539–557.

Wolock, D.M. and McCabe, G.J., 1995. Comparison and single and multiple flow direction algorithms for computing topographic parameters in TOPMODEL. *Water Resources Research*, 31 (5), 1315–1324.

Zhou, Q. and Liu, X., 2002. Error assessment of grid-based flow routing algorithms used in hydrological models. *International Journal of Geographical Information Science*, 16 (8), 819–842.